Drug Discovery Hot Paper

DOI: 10.1002/anie.201410341

# Application of Fragment-Based Screening to the Design of Inhibitors of *Escherichia coli* DsbA**

*Luke A. Adams, Pooja Sharma, Biswaranjan Mohanty, Olga V. Ilyichova, Mark D. Mulcair, Martin L. Williams, Ellen C. Gleeson, Makrina Totsika, Bradley C. Doak, Sofia Caria, Kieran Rimmer, James Horne, Stephen R. Shouldice, Mansha Vazirani, Stephen J. Headey, Brent R. Plumb, Jennifer L. Martin, Begoña Heras,* Jamie S. Simpson,* and Martin J. Scanlon**

**Abstract:** *The thiol-disulfide oxidoreductase enzyme DsbA catalyzes the formation of disulfide bonds in the periplasm of Gram-negative bacteria. DsbA substrates include proteins involved in bacterial virulence. In the absence of DsbA, many of these proteins do not fold correctly, which renders the bacteria avirulent. Thus DsbA is a critical mediator of virulence and inhibitors may act as antivirulence agents. Biophysical screening has been employed to identify fragments that bind to DsbA from Escherichia coli. Elaboration of one of these fragments produced compounds that inhibit DsbA activity in vitro. In cell-based assays, the compounds inhibit bacterial motility, but have no effect on growth in liquid culture, which is consistent with selective inhibition of DsbA. Crystal structures of inhibitors bound to DsbA indicate that they bind adjacent to the active site. Together, the data suggest that DsbA may be amenable to the development of novel antibacterial compounds that act by inhibiting bacterial virulence.*

Antibiotic resistance is a growing problem that has been recognized as one of the major health challenges of the 21st century.[1] With few antibacterials in the drug pipeline, new therapeutic targets and compounds with novel mechanisms of action are needed to treat resistant bacterial strains.[1b,d,2] One approach is to target bacterial virulence.[3] Antivirulence compounds are expected to exert less selective pressure, thus slowing down the development of resistance while sparing the normal host microbiota.[4] The development of antivirulence agents presents a number of challenges, and targeting virulence remains to be proven in a clinical setting. Nonetheless, compounds have been reported that inhibit virulence processes.[3c]

Many virulence factors produced by Gram-negative bacteria are secreted or surface-exposed proteins that are stabilized by disulfide bonds. Disulfide bond formation in the periplasm is catalyzed by enzymes of the Dsb (disulfide bond) family.[5] DsbA is a soluble enzyme of the thioredoxin superfamily that directly catalyzes disulfide bond formation in substrates.[6] DsbB is an all-α-helical integral membrane protein, which catalyzes reoxidation of DsbA.[7] The DsbA/DsbB system introduces disulfides bonds in a broad range of virulence factors and is therefore a central mediator of bacterial virulence.[5] Compounds that inhibit DsbB in biochemical assays have been reported, although their activity as antivirulence agents is unknown.[8] Genetic evidence has shown that Gram-negative bacteria lacking a functional DsbA are avirulent in animal infection models.[9] For example, mice infected with *Burkholderia pseudomallei*, the causative agent of melioidosis, all died when infected with a wild-type organism, but all survived when infected with a *dsbA*-deficient mutant.[10] Similarly, deletion of *dsbA* in uropathogenic *Escherichia coli* severely attenuated coloniza-

[*] Dr. L. A. Adams,[+] Dr. P. Sharma,[+] Dr. B. Mohanty, O. V. Ilyichova, Dr. M. D. Mulcair, Dr. M. L. Williams, E. C. Gleeson, Dr. B. C. Doak, Dr. S. Caria, Dr. K. Rimmer, Dr. J. Horne, M. Vazirani, Dr. S. J. Headey, B. R. Plumb, Dr. J. S. Simpson, Dr. M. J. Scanlon
Medicinal Chemistry, Monash Institute of Pharmaceutical Sciences, Monash University
381 Royal Parade, Parkville, VIC 3052 (Australia)
E-mail: jamie.simpson@monash.edu
martin.scanlon@monash.edu
Homepage: http://www.pharm.monash.edu.au

Dr. S. R. Shouldice, Prof. J. L. Martin, Dr. B. Heras[$]
Institute for Molecular Bioscience, University of Queensland
St. Lucia, QLD 4072 (Australia)

Dr. M. Totsika[#]
School of Chemistry and Molecular Biosciences
University of Queensland
St. Lucia, QLD 4072 (Australia)

[$] Present address: La Trobe Institute for Molecular Science, La Trobe University
Melbourne, VIC 3086 (Australia)
E-mail: b.heras@latrobe.edu.au

[#] Present address: Institute of Health and Biomedical Innovation, Queensland University of Technology
Kelvin Grove, QLD 4059 (Australia)

[+] These authors contributed equally to this work.

[**] We acknowledge funding from the National Health and Medical Research Council (grant number 1009785) and the Australian Research Council for an Australian Laureate Fellowship, a Future Fellowship, and a Discovery Early Career Researcher Award to J.L.M., B.H., and M.T., respectively (grant numbers FL0992138, FT130100580, and DE130101169). We thank the Bio21 Institute NMR Facility and the CSIRO Collaborative Crystallisation Centre (www.csiro.au/C3). This research was undertaken on the MX1 and MX2 beamlines at the Australian Synchrotron and at the UQ ROCX Diffraction Facility.

Supporting information for this article is available on the WWW under http://dx.doi.org/10.1002/anie.201410341.

  

tion of the mouse bladder.[11] The loss of virulence in *dsbA*-deficient mutants is attributed to misfolding and loss of function of DsbA substrates.

The central role of DsbA in bacterial virulence and our understanding of its catalytic mechanism make this enzyme an attractive target for the development of inhibitors. Crystal structures of DsbA have shown its mode of binding to substrates[12] and DsbB,[7] suggesting that it is amenable to structure-based approaches to the design of small-molecule inhibitors. However, inhibiting protein–protein interactions is often challenging.[13] In this context, the substrate-binding site of DsbA comprises a large hydrophobic groove rather than a well-defined binding pocket. Herein we report our approach to overcome these challenges by developing functional small-molecule inhibitors of *E. coli* DsbA (*Ec*DsbA), which to the best of our knowledge are the first reported nonpeptide inhibitors of DsbA.

We screened a library of 1132 fragments sourced from the Maybridge Ro3 collection to identify compounds that bind to oxidized *Ec*DsbA. The primary screen used saturation transfer difference (STD) NMR spectra with mixtures of three to five fragments.[14] Fragments with observable signals in STD-NMR spectra of the mixtures were retested as single compounds, as shown for phenylthiazole **1** (Figure 1a and b). In this way, 171 fragments were identified as hits from the STD-NMR screen.

Hits were validated by measuring chemical shift perturbations (CSP) for backbone amide resonances in $^{15}$N heteronuclear single quantum coherence (HSQC) spectra of $^{15}$N-labelled *Ec*DsbA upon addition of single fragments (1 mM). Under these conditions, 37 fragments produced CSP $\geq$ 0.01 ppm and were retained for further characterization. Each of the fragments caused CSP for residues in a hydrophobic groove of *Ec*DsbA (Figure 1c and d) that is adjacent to the active site and is implicated in the binding of *Ec*DsbA to both substrates and *Ec*DsbB. CSP analysis showed that none of the fragments had achieved saturation at the highest concentration tested (1 mM) indicating weak binding. Therefore, a preliminary fragment scoring system was devised based on the magnitude of CSP observed for residues in the hydrophobic groove of *Ec*DsbA that were unaffected by changes in DMSO concentration (Figure 2, see also Figures S1 and S2 in the Supporting Information).

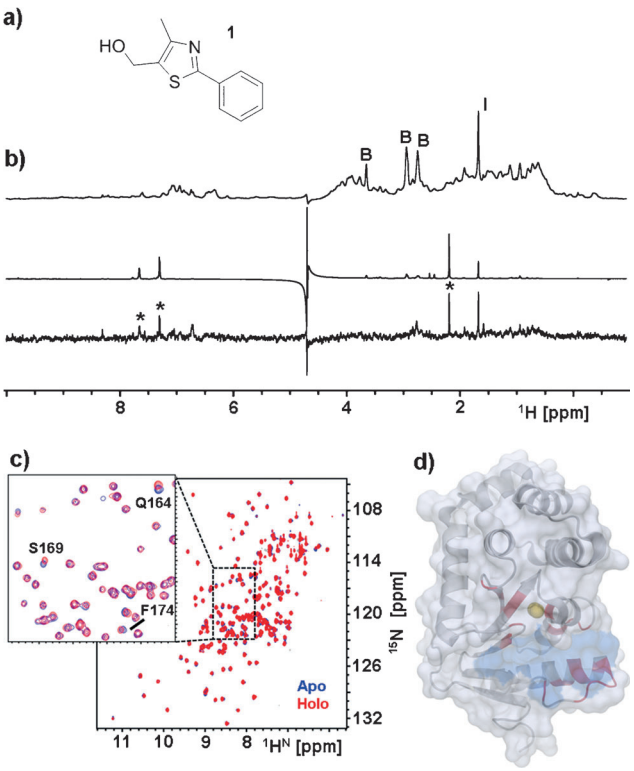


***Figure 1.*** Identification of fragments that bind *Ec*DsbA. a) STD-NMR showed that phenylthiazole **1** binds to *Ec*DsbA. b) (Top) $^1$H NMR spectrum of *Ec*DsbA; (middle) Off-resonance $^1$H NMR spectrum of *Ec*DsbA plus **1**; (bottom) STD-NMR spectrum of *Ec*DsbA plus **1**. STD signals from **1** are indicated (*); buffer peaks (B) and impurities (I) are labeled. c) Overlay of $^{15}$N HSQC spectra of *Ec*DsbA in the presence (red) and absence (blue) of **1** (1 mM). d) Residues with CSP $\geq$ 0.01 ppm in the HSQC spectrum are colored red on the structure of *Ec*DsbA (PDB ID: 1FVK). Also indicated are the active site (yellow sphere) and hydrophobic groove (blue).

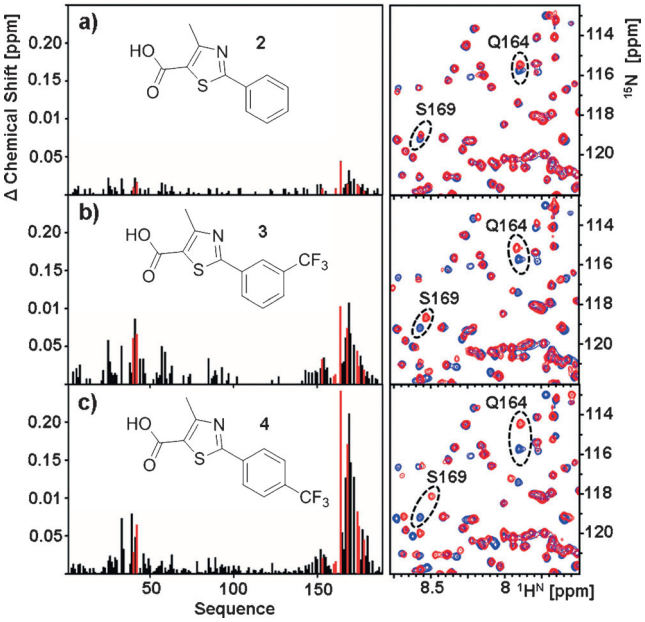


***Figure 2.*** Scoring of ligand binding to *Ec*DsbA. Left: Histogram of CSP per residue for unambiguously assigned residues of *Ec*DsbA induced by the compound shown. Hydrophobic groove residues are colored red. Right: Expansion of HSQC spectra highlighting perturbation of Gln164 and Ser169. The magnitude of CSP was used to score ligand binding as a) ligand **2** score = 1, b) ligand **3** score = 2, and c) ligand **4** score = 3.

The 37 fragments could be clustered into 8 distinct chemical classes and 11 singletons based on linear fingerprints (Figure 3 and S3). To expedite the initial evaluation of structure–activity relationships (SAR), singletons were set aside, and classes 1–5 were examined based on the obvious scaffold similarities within the clusters. Class 5 was deprioritized as an examination of other anilines in the library generated no clear SAR. Classes 1–4 were evaluated through

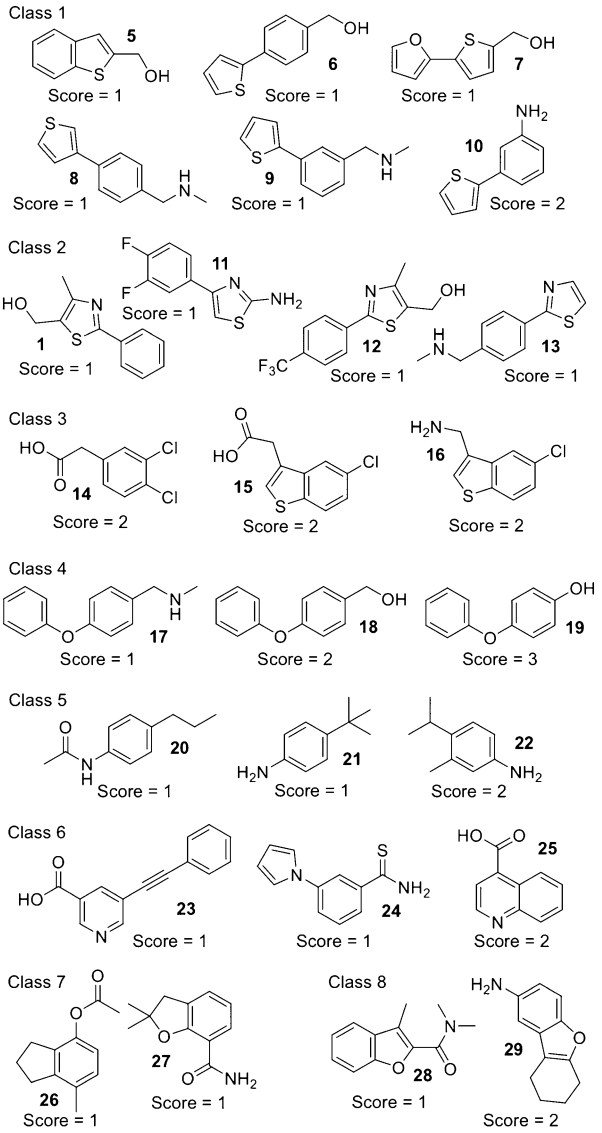


***Figure 3.*** Structures and HSQC score for the 26 fragment hits clustered using linear fingerprints into the 8 chemical classes shown.

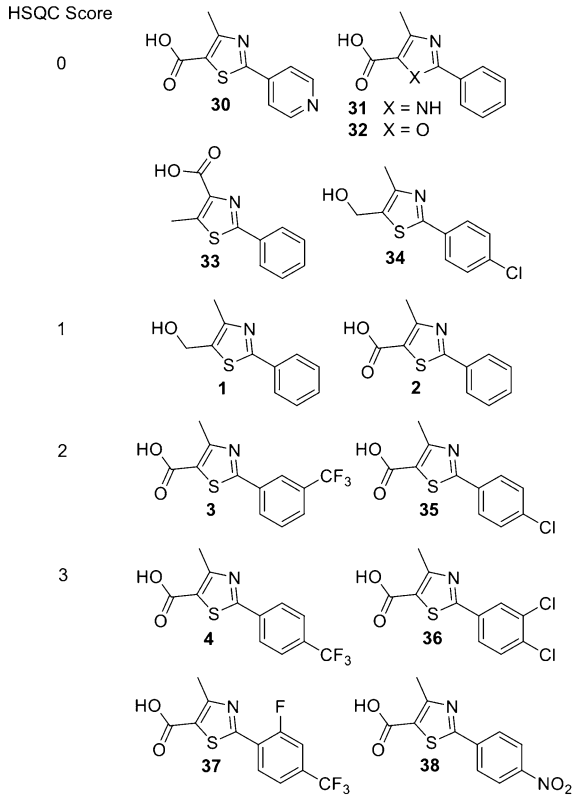


***Figure 4.*** Chemical structures and HSQC score for phenylthiazole analogues.

purchase and synthesis of analogues. Analysis of the binding of thiophenes in class 1 suggested multiple modes of binding to *Ec*DsbA, while analogues of the benzothiophenes of class 3 showed little improvement in binding as measured from their HSQC score, suggesting that progression of these classes was challenging. In contrast, the diphenyl ethers (class 4) and phenylthiazoles (class 2) both showed interpretable SAR, and are under development. The phenylthiazoles were prioritized because crystal structures of complexes were obtained for analogues in this class (see below) and the progression from phenylthiazole **1** is reported here.

Initially, 22 analogues of this scaffold were purchased and the HSQC score of each was determined (Figure 4 and S4). This produced initial SAR for the phenylthiazoles with the following trends. 2-Phenylthiazoles, in particular with halogen substituents on the aryl ring, were strongly favored (for example, fragments **4** and **36**). In contrast, replacing the phenyl ring with pyridine (**2** vs. **30**), led to a loss of detectable binding. Substitution of the thiazole **2** for either imidazole **31** or oxazole **32** had a detrimental effect on binding, as did inverting the methyl and acid substituents on the thiazole ring (**33**). Replacing the acid with the corresponding hydroxymethyl group (**35** vs. **34**) reduced solubility in some cases and thus gave conflicting SAR.

The phenylthiazole analogues (**4**, **36**, **37**, **38**) with the highest HSQC score were soaked into crystals of *Ec*DsbA, which resulted in one structure of the complex with compound **4** at 1.45 Å resolution. However, it was observed that two molecules of **4** were stacked in the hydrophobic groove of *Ec*DsbA (Figure S5; PDB ID: 4WF5). Therefore co-crystallization of **4** with *Ec*DsbA was undertaken, resulting in a structure with the expected 1:1 stoichiometry (Figure 5; PDB ID: 4WF4). In this structure, the thiazole formed a π–π stacking interaction with His32 and the aromatic ring was located in a hydrophobic pocket. The carboxy group at position 5 was orientated toward the more hydrophilic, water-filled portion of the hydrophobic groove.

Given the strong CSP in the HSQC spectrum and the available structural information, compound **4** was selected for further elaboration. A growth vector attached to the carboxy group of **4** was identified to enable extension along the hydrophobic groove of *Ec*DsbA. Preliminary studies into simple esters or amides identified these as poor analogues because of their lack of solubility in the aqueous buffer used for screening. Thus we chose to synthesize a series of amino acid derivatives to extend from the carboxy group at

  

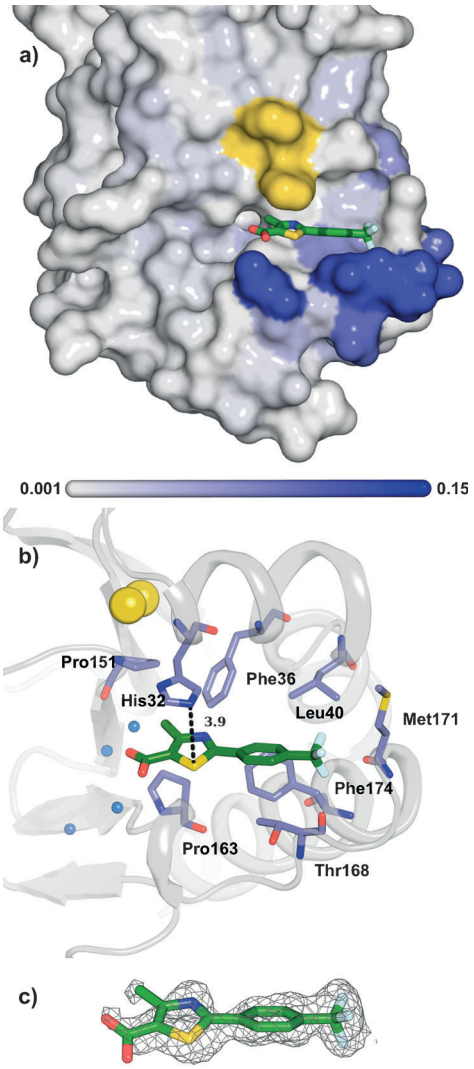


***Figure 5.*** Co-crystal structure of **4** bound to *Ec*DsbA. a) CSP observed in HSQC spectra upon addition of **4** are mapped onto the structure of *Ec*DsbA using a color gradient from white (< 0.001 ppm) to dark blue (≥ 0.15 ppm). Active-site residues Cys30–Cys33 are yellow. b) Phenylthiazole **4** (depicted as green sticks) binds within the hydrophobic groove of *Ec*DsbA. A π–π stacking interaction with His32 is indicated. Residues of *Ec*DsbA within 4 Å of **4** are shown as purple sticks and labeled. Water molecules are shown as blue spheres and the sulfur atoms of Cys30 and Cys33 are shown as yellow spheres. c) Simulated annealing omit $\sigma_A$-weighted mFo-DFc electron density maps contoured at 2.5 σ are shown as grey mesh.

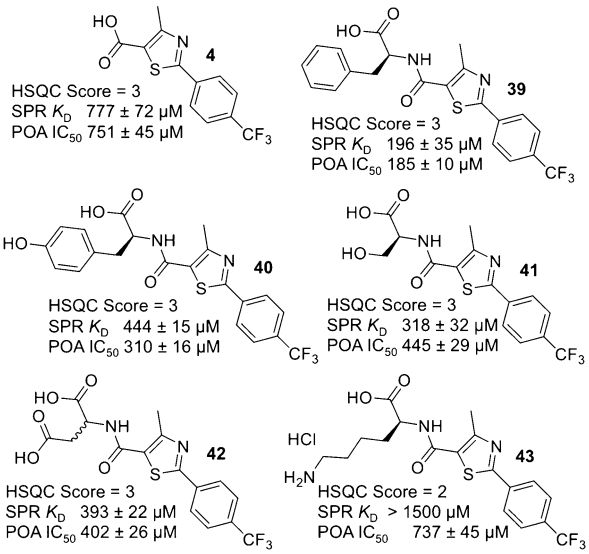


***Figure 6.*** HSQC score, binding affinity, and inhibitory concentration of selected amino acid derived ligands. $K_D$ and $IC_{50}$ values were determined by SPR and POA, respectively.

position 5, in order to explore chemical space while maintaining the solubilizing carboxylic acid group.

The binding affinity of these derivatives for *Ec*DsbA was evaluated using SPR. As shown in Figure 6 and Table S1, the $K_D$ values measured by SPR correlated well with the preliminary HSQC scores. The majority of compounds identified as strong hits by HSQC were observed by SPR to bind with $K_D$ values in the 200–400 μM range, while weaker HSQC hits gave $K_D$ values above 1 mM. The strongest binder was the phenylalanine derivative **39** with a $K_D$ value of 196 μM. Preliminary SAR suggested that aromatic (**39** and **40**) or short polar substituents (**41** and **42**) are more favorable, whereas lysine **43** proved detrimental to binding.

Inhibition of *Ec*DsbA activity was measured using a previously described peptide oxidation assay (POA).[15] Figures 6 and 7, Figures S7–S17, and Table S1 show that the inhibitory concentrations correlated well with the $K_D$ values determined by SPR.

The structure of **40** in complex with *Ec*DsbA at 1.63 Å resolution was determined from crystals prepared by co-crystallization (Figure 7d; PDB ID: 4WET). Unexpectedly, the tyrosine of **40** orientated perpendicular to the phenylthiazole core as opposed to extending along the hydrophobic groove. This structure showed two hydrogen-bond interactions from **40** to His32 and Gln164 of *Ec*DsbA (Figure 7e).

Compound **40** was tested for its ability to inhibit *Ec*DsbA in a bacterial motility assay.[12] As DsbA is not required for growth in rich media, but is essential for effective folding of the FlgI component of the bacterial flagella, the expected phenotype for an active *Ec*DsbA inhibitor is inhibition of *E. coli* motility, but no effect on growth. Addition of **40** (600 μM) in soft agar plates caused a 59% reduction in the zone of *E. coli* swarming motility compared to DMSO-containing control plates (Figure 7g), yet it had no effect on bacterial growth in liquid culture at 1 mM concentration (Figure 7h). Thus **40** was capable of inhibiting *Ec*DsbA in an isolated enzyme assay in vitro. In cell-based assays, **40** inhibited *E. coli* motility in soft agar, but had no effect on growth of *E. coli* in liquid media, which is consistent with selective inhibition of DsbA.

In conclusion, through a combination of fragment-based screening, biophysical assays, and X-ray structure determination, we have identified fragments that bind noncovalently to *Ec*DsbA and inhibit its activity. The fragments show concentration-dependent effects on *Ec*DsbA in biochemical (activity) and biophysical (binding) assays. Structural data indicate that the fragments occupy a hydrophobic groove

  

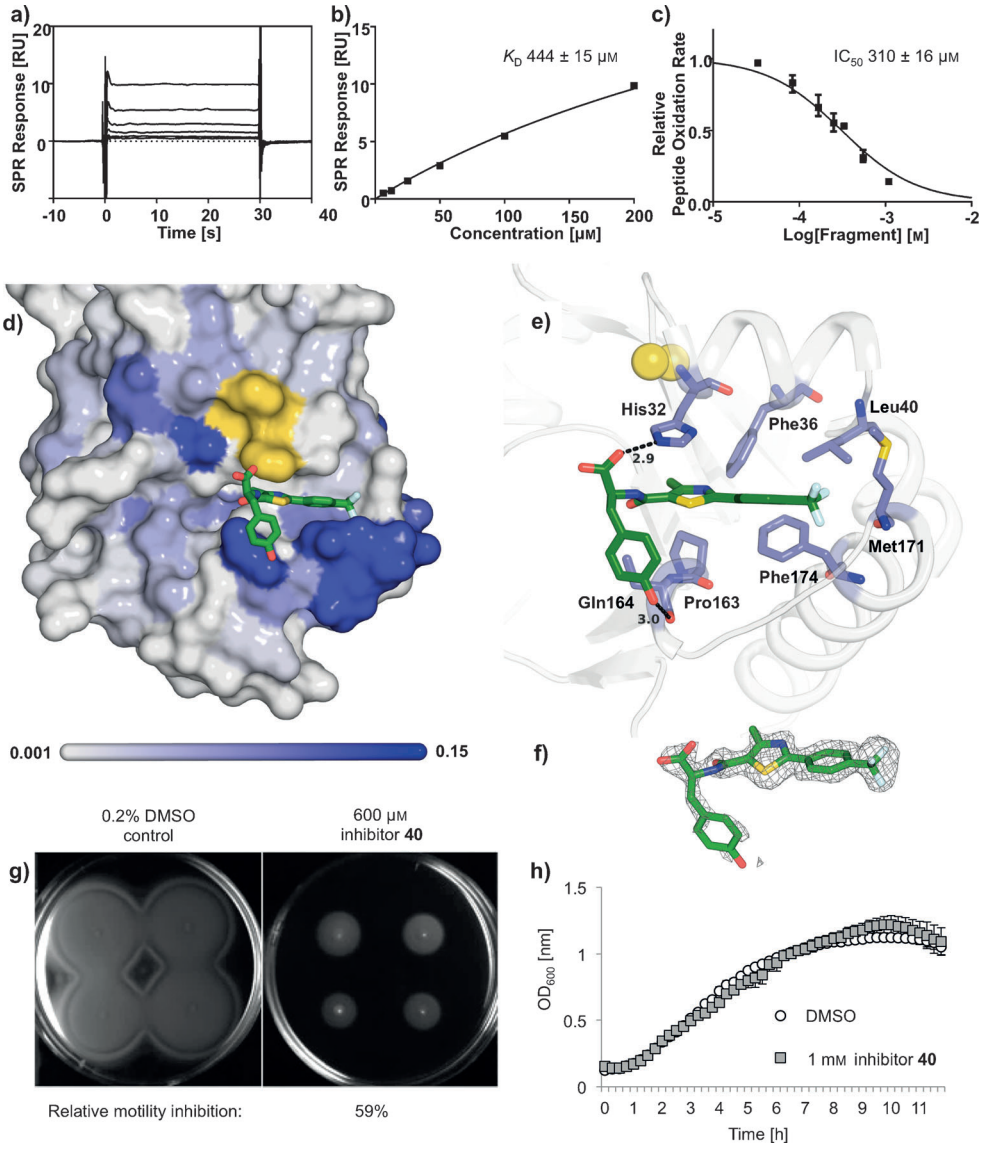


***Figure 7.*** Biochemical, structural, and phenotypic characterization of **40**. a) Raw sensorgrams and b) dose-response plot of **40** binding to *Ec*DsbA by surface plasmon resonance. c) Dose-dependent inhibition of *Ec*DsbA by **40** determined using a peptide oxidation assay. d) Crystal structure of **40** in complex with *Ec*DsbA. The surface is colored according to CSP observed in HSQC spectra of *Ec*DsbA upon addition of **40.** Active-site residues Cys30–Cys33 are colored yellow. e) Detailed view of the binding site for **40** on *Ec*DsbA. f) Simulated annealing omit $\sigma_A$-weighted mFo-DFc electron-density maps for **40** contoured at 2.5 σ are shown as grey mesh g) Motility of *E. coli* JCB816 on soft LB agar containing DMSO (left) and **40** (right). h) Growth of *E. coli* JCB816 in LB broth containing DMSO or **40**.

adjacent to the active site of *Ec*DsbA. Taken together, our data show that these compounds may represent a starting point for the development of antivirulence agents that inhibit *Ec*DsbA. Compounds with this spectrum of activity may exert less selective pressure than traditional antibiotics that kill bacteria or inhibit their growth, thus slowing down the development of resistance, and could therefore represent a future treatment of multi-drug resistant bacterial infections.[3c]

Received: October 22, 2014
Revised: November 25, 2014
Published online: December 30, 2014

**Keywords:** bacterial virulence · drug design · *Ec*DsbA · fragment-baseddrugdiscovery· medicinal chemistry

[1] a) M. A. Cooper, D. Shlaes, *Nature* **2011**, *472*, 32; b) B. Obama, *Executive Order—Combating antibiotic-resistant bacteria*, http://www.whitehouse.gov/the-press-office/2014/09/18/executive-order-combating-antibiotic-resistant-bacteria; c) R. R. Uchil, G. S. Kohli, V. M. Katekhaye, O. C. Swami, *J. Clin. Diagn. Res.* **2014**, *8*, ME01–04; d) World Health Organization in *Antimicrobial resistance: global report on surveillance 2014*; e) G. D. Wright, *Chem. Biol.* **2012**, *19*, 3–10.

[2] J. Fernebro, *Drug Resist. Updates* **2011**, *14*, 125–139.

[3] a) R. C. Allen, R. Popat, S. P. Diggle, S. P. Brown, *Nat. Rev. Microbiol.* **2014**, *12*, 300–308; b) B. Heras, M. J. Scanlon, J. L. Martin, *Br. J. Clin. Pharmacol.* **2014**, DOI: 10.1111/bcp.12356; c) D. A. Rasko, V. Sperandio, *Nat. Rev. Drug Discovery* **2010**, *9*, 117–128.

[4] a) A. K. Barczak, D. T. Hung, *Curr. Opin. Microbiol.* **2009**, *12*, 490–496; b) A. E. Clatworthy, E. Pierson, D. T. Hung, *Nat. Chem. Biol.* **2007**, *3*, 541–548; c) S. A. Stanley, D. T. Hung, *Biochemistry* **2009**, *48*, 8776–8786; d) M. Zucca, S. Scutera, D. Savoia, *Mini-Rev. Med. Chem.* **2011**, *11*, 888–900.

[5] B. Heras, S. R. Shouldice, M. Totsika, M. J. Scanlon, M. A. Schembri, J. L. Martin, *Nat. Rev. Microbiol.* **2009**, *7*, 215–225.

[6] J. L. Martin, J. C. Bardwell, J. Kuriyan, *Nature* **1993**, *365*, 464–468.

[7] K. Inaba, S. Murakami, M. Suzuki, A. Nakagawa, E. Yamashita, K. Okada, K. Ito, *Cell* **2006**, *127*, 789–801.

[8] V. Früh, Y. Zhou, D. Chen, C. Loch, E. Ab, Y. N. Grinkova, H. Verheij, S. G. Sligar, J. H. Bushweller, G. Siegal, *Chem. Biol.* **2010**, *17*, 881–891.

[9] T. Miki, N. Okada, H. Danbara, *J. Biol. Chem.* **2004**, *279*, 34631–34642.

  

[10] P. M. Ireland, R. M. McMahon, L. E. Marshall, M. Halili, E. Furlong, S. Tay, J. L. Martin, M. Sarkar-Tyson, *Antioxid. Redox Signaling* **2014**, *20*, 606 – 617.
[11] M. Totsika, B. Heras, D. J. Wurpel, M. A. Schembri, *J. Bacteriol.* **2009**, *191*, 3901 – 3908.
[12] J. J. Paxman, N. A. Borg, J. Horne, P. E. Thompson, Y. Chin, P. Sharma, J. S. Simpson, J. Wielens, S. Piek, C. M. Kahler, H. Sakellaris, M. Pearce, S. P. Bottomley, J. Rossjohn, M. J. Scanlon, *J. Biol. Chem.* **2009**, *284*, 17835 – 17845.
[13] T. L. Nero, C. J. Morton, J. K. Holien, J. Wielens, M. W. Parker, *Nat. Rev. Cancer* **2014**, *14*, 248 – 262.
[14] M. Mayer, B. Meyer, *Angew. Chem. Int. Ed.* **1999**, *38*, 1784 – 1788; *Angew. Chem.* **1999**, *111*, 1902 – 1906.
[15] F. Kurth, K. Rimmer, L. Premkumar, B. Mohanty, W. Duprez, M. A. Halili, S. R. Shouldice, B. Heras, D. P. Fairlie, M. J. Scanlon, J. L. Martin, *PLoS One* **2013**, *8*, e80210.

  